

The CMS Tracker performance in LHC Run 3

Tomáš Kello on behalf of the CMS Collaboration^{a,*}

^a*INFN Florence*

E-mail: tomas.kello@cern.ch

The Tracker of the Compact Muon Solenoid (CMS) experiment is the largest silicon tracker ever built, with 1856 pixel and 15148 strip detector modules that provide accurate track reconstruction. Special challenges must be addressed in the Run 3 data-taking period such as the high instantaneous luminosity and the rapid changes due to module irradiation, particularly in the newly installed Layer 1 of the barrel pixel detector. To achieve high precision in measurements of the momenta of charged particles, corrections for the position, rotation and curvature of the detector modules must be found; a procedure known as tracker alignment. Magnet cycles, temperature variations and aging of modules cause significant time variations that affect the track reconstruction and therefore necessitate continuous alignment throughout the operation of the Large Hadron Collider (LHC) machine. In this paper, the performance of the CMS Tracker pixel and strip detectors on early Run 3 data will be presented. Focus will also be placed on the CMS Tracker alignment, highlighting new features developed for the Run 3 data taking period. The impact of the Tracker alignment on physics performance will also be reviewed.

*6th International Conference on Technology and Instrumentation in Particle Physics (TIPP2023)
4 - 8 Sep 2023
Cape Town, Western Cape, South Africa*

*Speaker

1. Introduction

The CMS detector is a general-purpose particle detector situated at CERN that utilizes its cylindrical geometry and magnetic field of 3.8 T to facilitate precise measurements of particles arising from the high energy particle interactions at the LHC [1]. The CMS Tracker, 5.8 m long and 2.5 m in diameter, is situated in the immediate proximity from the interaction point. It was designed to reconstruct trajectories (also called tracks) of electrically charged particles traversing the detector volume with an ultimate resolution, enabling precise measurement of the particles momenta and impact parameters. It consists of two main detection sub-systems: the silicon Pixel Tracker (Figure 1 left) and the silicon Strip Tracker (Figure 1 right).

The silicon Pixel Tracker is the innermost CMS component. As such, it is exposed to the extreme operational conditions caused by the high particle flux, e.g. 600 MHz/cm² for the Layer 1. A current version of the Pixel Tracker, known as Phase-1 upgrade [2], consists of 1856 modules, accounting for over 124 million pixels with a size of $150 \times 100 \mu\text{m}^2$. Pixel modules are situated in four concentric barrel layers (BPIX) and three forward disks (FPIX). To improve the quality of the collected data, it was necessary to refurbish the CMS pixel detector, namely to fully exchange BPIX Layer 1, revise FPIX high-voltage power distribution scheme and replace all the DC-DC converter modules with new modules featuring an improved FEAST2.3 ASIC [3]. The aim was also to help to adapt for the growing number of the instantaneous delivered luminosity (from $1.8 \times 10^{34} \text{cm}^{-2} \text{s}^{-1}$ by the end of LHC Run 2 to $2.1 \times 10^{34} \text{cm}^{-2} \text{s}^{-1}$ measured in the beginning of LHC Run 3), and an average number of interactions per bunch crossing (pile-up), rising from an average of 37 interactions per bunch crossing at the end of LHC Run 2 to 52 interactions per bunch crossing in 2023.

The silicon Strip Tracker extends the radial coverage from 20 to 116 cm, providing at least 9 single point measurements within the $|\eta| < 2.4$ pseudorapidity range. In the barrel region, ten layers of strip modules surround the pixel detector, four of them in the Tracker Inner Barrel (TIB) and six in the Tracker Outer Barrel (TOB). Complementary to the layers in the inner region, three Tracker Inner Disks (TID) are situated at each side of TIB. The silicon strip coverage in the forward region is then provided by Tracker EndCaps (TEC) consisting of nine disks at each side. In total, 15 148 silicon strip modules are used, differing in the shape and thickness of the sensors. The latter is specified to 320 μm in TIB, TID and in rings 1-4 in TEC disks, while 500 μm thick sensors are used in TEC rings 5-7. Four barrel layers and three endcap rings contain so-called stereo modules, for which an additional strip sensor is attached back-to-back to the first sensor with a small stereo angle of 100 mrad allowing for a measurement of an additional coordinate, z in the barrel and r in the endcap. A definition of the global CMS coordinate system used in this paper can be found in Ref. [1].

The performance of both CMS Pixel [6, 7] and Strip [8, 9] detectors was studied using the early LHC Run 3 data sets and is presented in Section 2 and 3. The performance of the CMS Tracker alignment [10–12] derived at the beginning of LHC Run 3 is summarised in Section 4.

2. The CMS pixel detector performance

The precise position of the charged particle hit in the pixelated silicon detector is interpolated from the charge distribution in the cluster formed by adjacent pixels with a deposited charge above

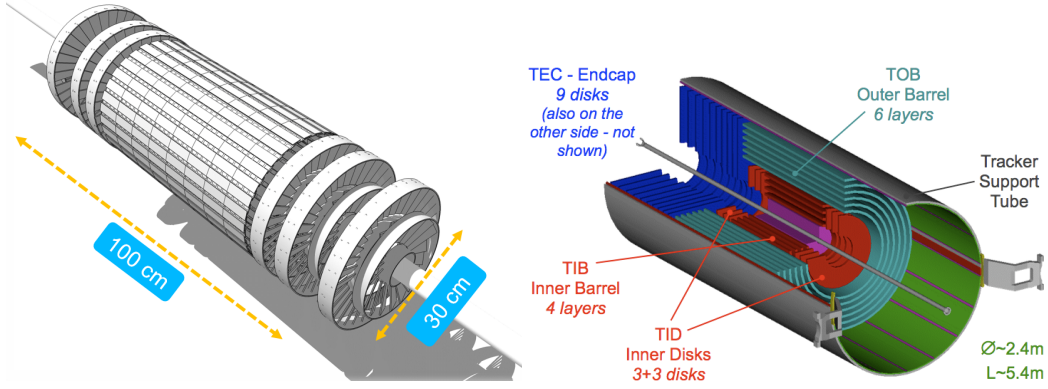


Figure 1: A sketch of the CMS silicon Pixel Tracker [4] (left) and the CMS silicon Strip Tracker [5] (right).

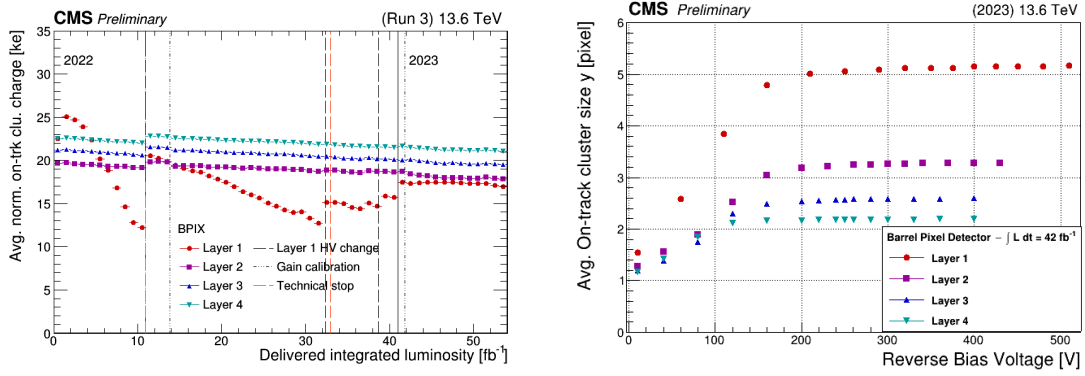


Figure 2: The historic trend of the normalized on-track cluster charge (Norm. on-trk. clu. charge [ke]) in each barrel pixel (BPIX) layer is shown as a function of delivered integrated luminosity (left). A full bias scan performed at the beginning of 2023 data taking is shown for all BPIX layers while the average on-track cluster size in the local y direction (Avg. On-track cluster size y), i.e. global z coordinate, is monitored (right).

certain threshold. The charge collection efficiency in the pixels is severely affected by radiation damage, therefore it is necessary to monitor the cluster properties, e.g. by measuring an average cluster charge and size. A historic trend in Figure 2 (left) shows the average cluster charge (normalized by an incidence angle) as measured since the beginning of LHC Run 3 until July 2023. Continuous negative inclination of the trend, mostly visible for the first BPIX layer, is a sign of radiation damage. To tackle this issue, an increasingly higher operational bias voltage is applied for the affected sensors, typically during LHC machine technical or year-end stops. A beneficial effect of annealing can also be seen for the other BPIX layers at around 11 fb^{-1} of delivered integrated luminosity. To determine the optimal operational bias voltage for pixels, the average cluster size in local x , i.e. global $r - \Phi$ coordinate, and local y direction, i.e. global z coordinate on the barrel and global r coordinate on the endcap, is monitored (see Figure 2 right), and a working point is chosen from the plateau region. In this example, the operational bias voltage at a working point for BPIX Layer 1 was gradually increased from 150 V and was eventually set to 400 V (as of the end of July 2023).

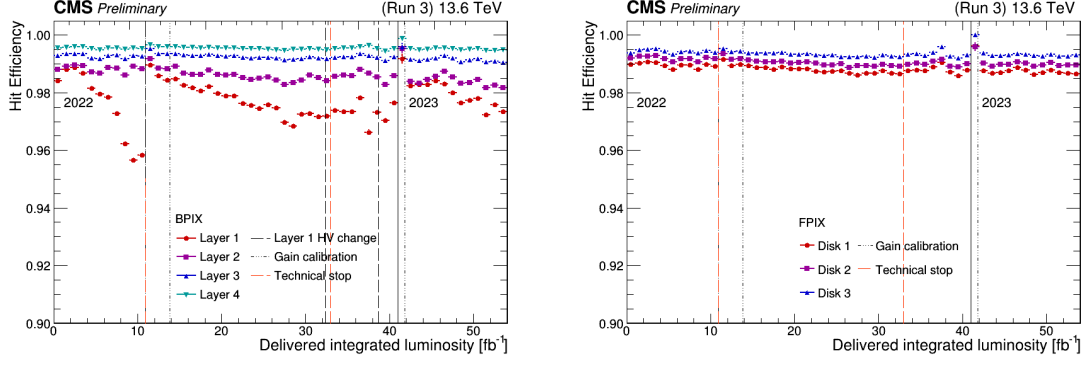


Figure 3: The historic trend of the Pixel Tracker hit efficiency measured in the beginning of LHC Run 3 as a function of delivered integrated luminosity. Results are shown independently for all layers in the barrel pixel (left) and all disks in the forward pixel (right).

Another important quantity in the monitoring of the Pixel Tracker performance is the hit efficiency. It is defined as a probability to find any pixel cluster within 1 mm around an expected hit (independent of the cluster quality), while all modules marked as bad are excluded from this measurement. At the beginning of LHC Run 3, the hit efficiency for the most exposed BPIX Layer 1 reached values in excess of 96%. Values greater than 98% were monitored for the rest of BPIX layers as well as all FPIX disks, as can also be observed from the historic trends in Figure 3. Given the challenging conditions resulting from an instantaneous luminosity of $2.1 \times 10^{34} \text{cm}^{-2} \text{s}^{-1}$, the hit efficiency is competitive to that achieved during LHC Run 2 [4].

3. The CMS strip detector performance

Unlike the silicon Pixel Tracker, the silicon Strip Tracker is in operation without any major adjustments of its geometry since the commissioning of the CMS detector in 2007. At the beginning of LHC Run 3 in 2022 (corresponding to the total integrated luminosity of about 205fb^{-1}), a drop in the fraction of bad detector modules by 0.5% has occurred thanks to the recovery of a cooling loop in the TEC. Consequently, the fraction of active detector components has remained stable at 96% throughout the beginning of the LHC Run 3 period up to the end of June 2023, corresponding to 254.6fb^{-1} .

The strip hit efficiency was measured with $\sqrt{s} = 13.6 \text{ TeV}$ data collected in 2022, using both standard fills with the instantaneous delivered luminosity under $1.8 \times 10^{34} \text{cm}^{-2} \text{s}^{-1}$ and high luminosity fills above this value. The hit efficiency in the TOB (TIB) was found to be greater than $> 97.5\%$ ($> 98.5\%$) depending on the particular barrel layer, as can also be observed from Figure 4. The bad detector components were not included in this measurement.

A high signal-to-noise ratio (S/N) for the strip sensors ensures a good zero suppression and a proper strip cluster build-up. The S/N values decrease with a fluence, therefore they decrease linearly with integrated luminosity as shown in the historic trends for LHC Run 2 and the beginning of LHC Run 3 in Figure 5 (left). Applying an extrapolation to 500fb^{-1} (approximate end of CMS Run 3 operation), we expect a decrease in the S/N values to 18.5 (14.5) for the $500 \mu\text{m}$ ($320 \mu\text{m}$) thick sensors.

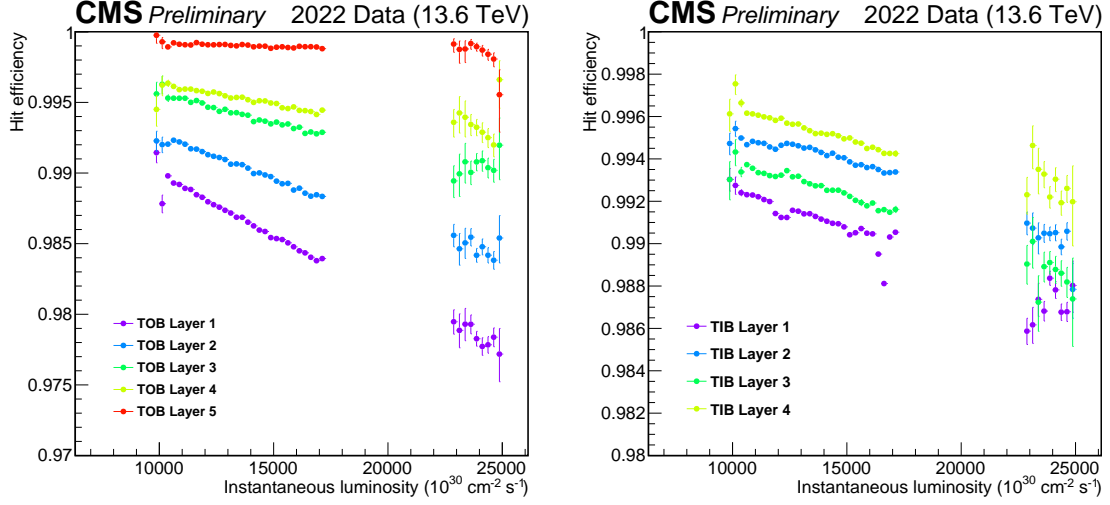


Figure 4: Hit efficiency of silicon strip detectors from five TOB layers (left) and four TIB layers (right) as a function of instantaneous luminosity.

The strip hit resolution is computed employing the so-called pair method [13]. In this method, hit pairs are selected from overlapping sensors where the following requirements are fulfilled: a cluster width of at most four strips; the clusters in the pair have the same width; only pairs within the same layer are allowed (i.e. distance of propagation from one surface to the next is < 7 cm and error in the bending coordinate between the two hits is $< 25 \mu\text{m}$). Tracks selected for this study have the transverse momentum component $p_T > 3$ GeV, number of hits ≥ 6 and $\chi^2 \geq 1$. Hit resolution results for different cluster widths are shown in Figure 5 (right). The fact that all measurements are better than binary resolution with $\text{pitch}/\sqrt{12}$ demonstrates the benefit from charge sharing with analogue readout.

4. The CMS Tracker alignment performance

4.1 Tracker alignment

The CMS Tracker was designed to provide measurements of charged particle trajectories (tracks) with a hit resolution of $O(10 \mu\text{m})$. In reality, the limitations arising from the nature of the mechanical installment of tracker components unavoidably reduce the hit resolution to a suboptimal $O(100 \mu\text{m})$. To tackle this issue, dedicated algorithms (also known as tracker alignment) are in place to derive necessary corrections to the position, orientation and surface deformation of the silicon modules. Moreover, an accurate and timely derivation of alignment parameters is of utmost importance to account for unavoidable movements inside the detector. In particular, two magnet cycles (one from fault) in 2022, and eight magnet cycles (seven from fault) occurred by the end of 2023, causing detector movements of $O(1 \text{ mm})$ magnitude. Besides that, effects of temperature variation during the cooling cycle (typically movements of the order $O(10 \mu\text{m})$), and effects of sensor aging due to the high radiation levels (typically $O(1 \mu\text{m})$) need to be taken into account.

The Tracker alignment procedure can be essentially narrowed down to the track-hit residual

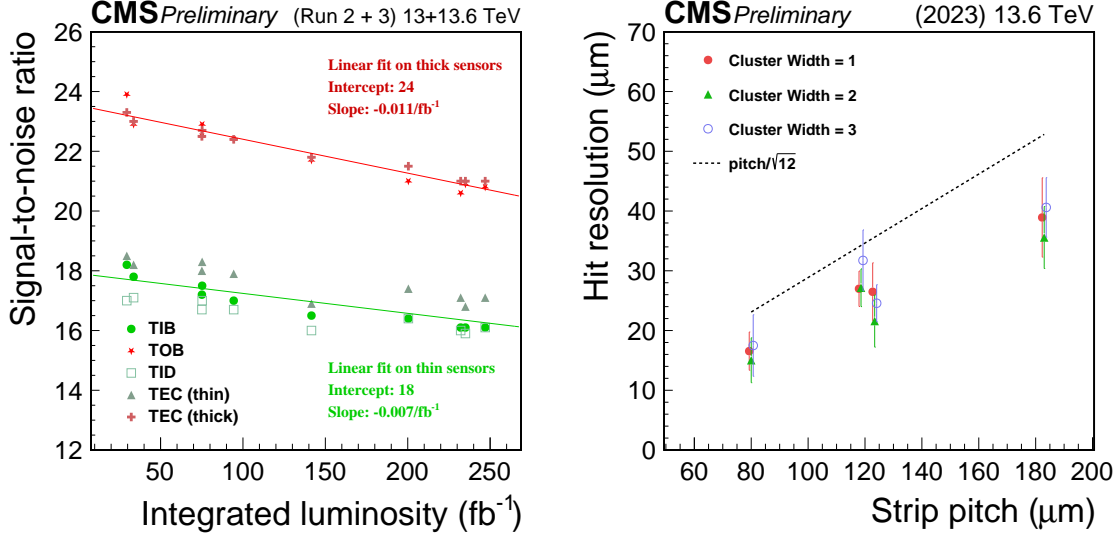


Figure 5: The signal-to-noise ratio (S/N) measured in pp collisions since LHC Run 2 is shown as a function of the integrated delivered luminosity (left) both for the 500 μm (red) and 320 μm (green) thick sensors. The strip hit resolution for different cluster widths was measured using LHC Run 3 pp collisions and is also reported (right). The binary resolution for $\text{pitch}/\sqrt{12}$ is also shown (dotted line).

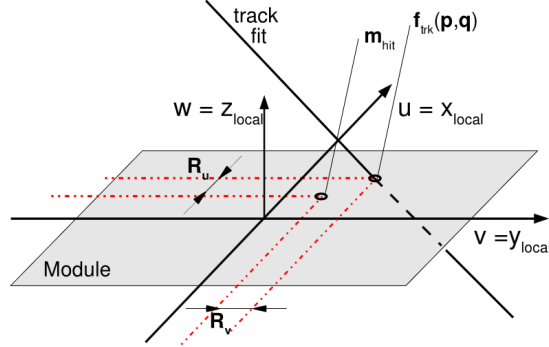


Figure 6: The definition of the track-hit residual $m_{\text{hit}} - f_{\text{trk}}(\vec{p}, \vec{q})$ in the local x and y coordinates. [15]

minimisation problem (see Figure 6) for the χ^2 function defined as:

$$\chi^2(\vec{p}, \vec{q}) = \sum_j^{\text{tracks}} \sum_i^{\text{hits}} \left(\frac{m_{ij} - f_{ij}(\vec{p}, \vec{q}_j)}{\sigma_{ij}^m} \right)^2, \quad (1)$$

where \vec{p} is a complete set of all assumed alignment parameters describing the detector's geometry, \vec{q} stands for the complete set of all track parameters (e.g. curvature), $m_{ij} \pm \sigma_{ij}$ represents the measurement (e.g. hits) with the corresponding uncertainty (e.g. local hit resolution) and f_{ij} stands for a prediction (i.e. trajectory obtained in a fit assuming \vec{p} and \vec{q} values). Results presented in this text were produced employing MILLE-PEDE-II [14] software and its derivations developed as a particular solution to this multiparametric minimisation problem.

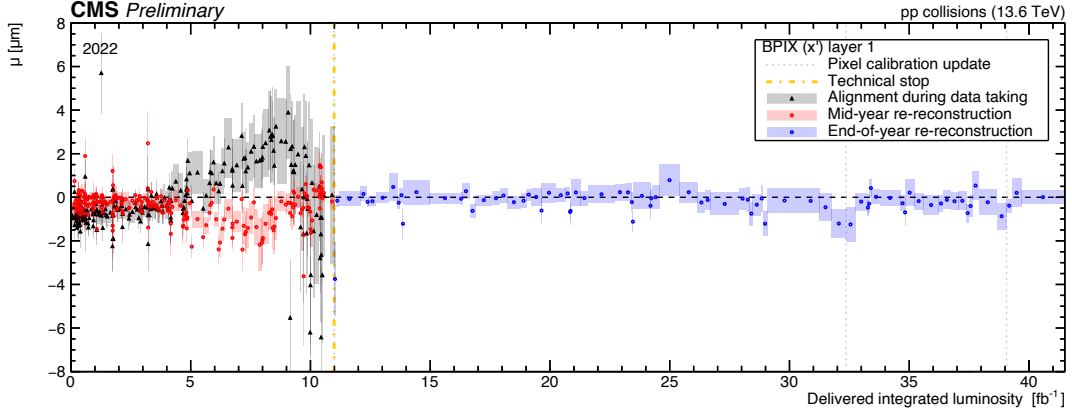


Figure 7: The mean value of the distribution of median residuals is plotted for the local x (x') direction in the first BPIX layer as a function of the delivered integrated luminosity. The vertical grey dotted lines indicate a change in the Pixel Tracker calibration and the yellow line, a 4 week technical stop. The uncertainty corresponds to the standard mean error of the displayed quantity.

4.2 Alignment performance in the beginning of LHC Run 3

Depending on the nature of tracker internal movements, an abundance of the collected data sets and an urgency of the alignment corrections it is possible (and often necessary) to align detector at the higher-level structures (HLS), such as half-barrels or ladders in BPIX, instead of more granular and time consuming module-level (ML) alignment. Figure 7 shows a time evolution of the alignment performance expressed by a mean μ of the Distribution of Median track-hit Residuals (DMR) as a function of delivered integrated luminosity during 2022. An ideally aligned tracker would have $\mu = 0$ and show narrow DMR width. Data points in black correspond to the automated low-granularity alignment workflow that only aligns CMS Pixel Tracker at the level of half-barrels (BPIX) and half-cylinders (FPIX). Alignment conditions were consequently refined in dedicated offline re-reconstruction (red points up to 9 fb^{-1}) by increasing granularity of the alignment as well as using all available data sets of pp collisions and cosmic rays. An important milestone was reached about 2 fb^{-1} of integrated luminosity before the technical stop in 2022 when the high-granularity (HG) automated workflow was activated for the first time. It was designed to align the Pixel Tracker at the level of ladders (BPIX) and panels (FPIX) with the strip detector fixed. The HG workflow remained activated (blue points) and showed superior performance for the rest of the data-taking in 2022 ($\approx 30 \text{ fb}^{-1}$).

The alignment parameters derived in 2022 served as a starting geometry for the alignment efforts in 2023. In this paper, three sets of alignment conditions derived at the end of June 2023 are reported (Figure 8): the first alignment in 2023 with cosmic rays collected at 3.8 T magnetic field (green); the alignment with cosmic rays and pp collisions at center of mass energy of 900 GeV (blue); and, the alignment with cosmic rays and pp collisions at center of mass energy of 13.6 TeV (red). Due to the limited number of tracks, the prompt alignment with solely cosmic ray data sets was performed at the level of ladders for BPIX, while the HLS alignment with half-cylinders was used in case of FPIX. The Strip Tracker partitions were aligned at the level of half-barrels and half-cylinders. Alignment at $\sqrt{s} = 900 \text{ GeV}$ was performed at the ML for the Pixel Tracker while the strip

detector was kept fixed. Alignment at $\sqrt{s} = 13.6$ TeV used around 16 million pp collision tracks and 295,000 cosmic ray tracks. Coarser alignment was performed at the level of ladders and panels for the pixel detector and with the strip detector fixed. Performance of all three geometries was validated in the measurement of DMRs for all Tracker partitions and is displayed for comparison for BPIX and FPIX in Figure 8. Physics performance of the Tracker was evaluated from the mean values of the distributions of the unbiased track-vertex residuals in the transverse plane, d_{xy} , and longitudinal direction, d_z . In case of a perfectly performed calibration, mean values of zero are expected. Both an effect of the higher granularity of the alignment and an abundance of available tracks used in the fit have contributed to the improved physics performance, as can be seen in Figure 9 for the alignment with $\sqrt{s} = 900$ GeV and $\sqrt{s} = 13.6$ TeV data sets, respectively.

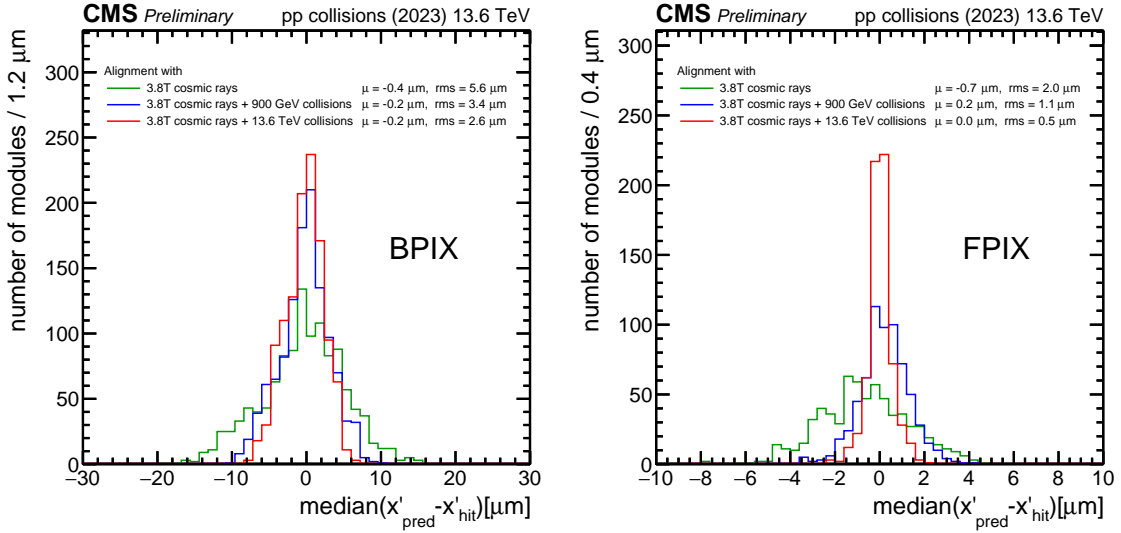


Figure 8: The distribution of median residuals is shown for the local x (x') direction in the barrel pixel detector (BPIX), evaluated using pp collision tracks collected at $\sqrt{s} = 13.6$ TeV. Comparison of three sets of alignment parameters derived in 2023 is displayed and is further explained in text. The quoted means μ and root-mean-squares (rms) are the parameters of a Gaussian fit to the distributions.

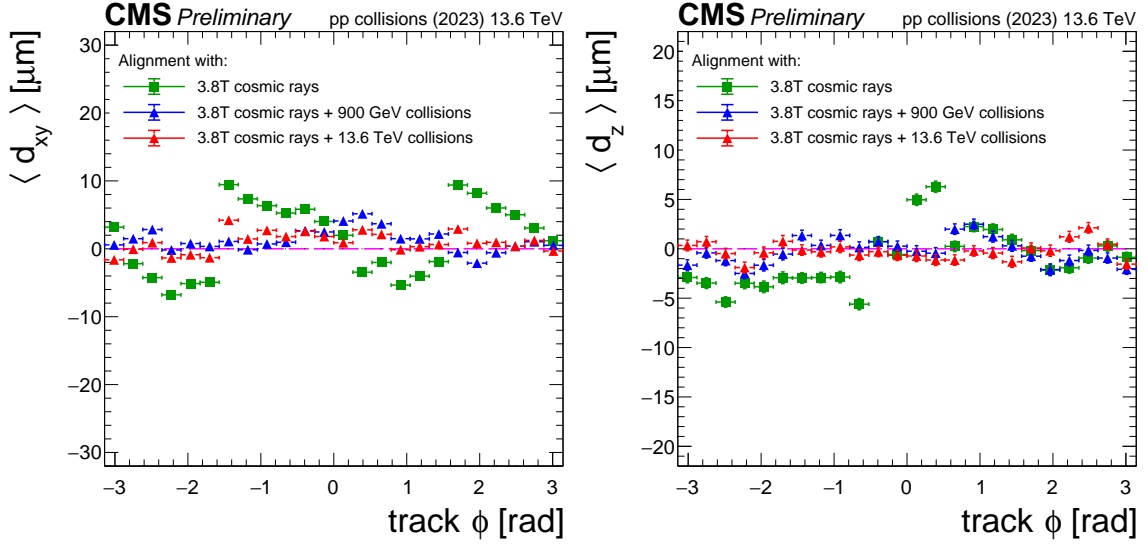


Figure 9: The distance in the transverse plane (left) and in the longitudinal direction (right) of the tracks at their point of closest approach to a refit unbiased primary vertex is studied in bins of track azimuthal angle using a sample of collision events collected by the CMS detector at full magnetic field (3.8T) during pp collisions data taking at $\sqrt{s} = 13.6$ TeV, selected online through minimum bias triggers. Comparison of three sets of alignment parameters derived in 2023 is displayed and is further explained in text. The residual deviations from the ideal case (purple dashed line, mean of 0) show the typically achieved precision of the alignment. Vertical error bars represent the statistical uncertainty due to the limited number of tracks, which can be smaller than the size of the markers.

5. Conclusions

The CMS Tracker has entered LHC Run 3 operations facing the challenging conditions formed by instantaneous luminosity of $2.1 \times 10^{34} \text{cm}^{-2}\text{s}^{-1}$ and increased pile-up values. First measurements of the Tracker performance are showing its excellent state and predict its nominal operation until the end of Run 3. While aging of the Tracker is visible, a robust monitoring allows for an active intervention. Excellent results with both offline and automated alignment workflows were shown while more dedicated alignment efforts are yet to come.

References

- [1] CMS Collaboration. The CMS experiment at the CERN LHC. *Journal of Instrumentation*, 3(08):S08004, Aug 2008. [10.1088/1748-0221/3/08/S08004](https://doi.org/10.1088/1748-0221/3/08/S08004).
- [2] The Tracker Group of the CMS Collaboration. The CMS Phase-1 pixel detector upgrade. *Journal of Instrumentation*, 16(02):P02027, Feb 2021. [10.1088/1748-0221/16/02/P02027](https://doi.org/10.1088/1748-0221/16/02/P02027).
- [3] Lars O. S. Nohte on behalf of the Tracker Group of the CMS Collaboration. CMS Phase-1 pixel detector refurbishment during LS2 and readiness towards the LHC Run 3. *Journal of Instrumentation*, 17(09):C09017, Sep 2022. [10.1088/1748-0221/17/09/C09017](https://doi.org/10.1088/1748-0221/17/09/C09017).
- [4] Tamas Almos Vami on behalf of the Tracker Group of the CMS Collaboration. Calibration and performance of the CMS pixel detector in LHC Run 2. 2019. [10.48550/arXiv.1909.12920](https://arxiv.org/abs/1909.12920).

- [5] Giacomo Sguazzoni on behalf of the CMS Silicon Strip Tracker Collaboration. The construction and commissioning of the CMS Silicon Strip Tracker. 2008. [10.48550/arXiv.0809.3344](#).
- [6] CMS Collaboration. Pixel Detector Performance in Run 3. 2022. [CMS-DP-2022-067](#).
- [7] CMS Collaboration. Pixel Detector Performance in early 2023. 2023. [CMS-DP-2023-041](#).
- [8] CMS Collaboration. CMS Silicon Strip Tracker Performance Results in 2022. 2023. [CMS-DP-2023-030](#).
- [9] CMS Collaboration. CMS Silicon Strip Tracker Performance in 2023. 2023. [CMS-DP-2023-040](#).
- [10] CMS Collaboration. Tracker Alignment Performance in 2022. 2022. [CMS-DP-2022-044](#).
- [11] CMS Collaboration. Tracker alignment performance in 2022 (addendum). 2022. [CMS-DP-2022-070](#).
- [12] CMS Collaboration. Tracker alignment performance in early 2023. 2023. [CMS-DP-2023-039](#).
- [13] Erik Butz on behalf of the CMS Collaboration. Operation and Performance of the CMS outer tracker. *PoS, Vertex* 2017:013, 2018. [10.22323/1.309.0013](#).
- [14] Volker Blobel and Claus Kleinwort. A New method for the high precision alignment of track detectors. In *Conference on Advanced Statistical Techniques in Particle Physics*, June 2002. [10.48550/arXiv.hep-ex/0208021](#).
- [15] Marco Musich. *The Alignment of the CMS Tracker and its Impact on the Early Quarkonium Physics*. PhD thesis, Turin U., 2011. [CERN-THESIS-2011-435](#).